Alméras *et al. Annals of Forest Science* (2025) 82:15
https://doi.org/10.1186/s13595-025-01284-9

Annals of Forest Science

RESEARCH Open Access

The diversity of radial variations of wood properties in European beech (*Fagus sylvatica* L.) reveals the plastic nature of juvenile wood

Tancrède Alméras[1], Delphine Jullien[1], Shengquan Liu[2], Caroline Loup[3], Joseph Gril[4,5*] and Bernard Thibaut[1]

Abstract

Key message Radial variations in wood quality result from the changes in wood properties with tree age. Here, we show that, at least in beech (*Fagus sylvatica* L.), these patterns of variations are diverse, and reflect a plastic adaptation to changes in the mechanical needs of the trees during their life.

Context The radial variation of wood properties in the young age of the tree can be interpreted as the result of either cambium ageing (ontogenetic juvenility) or adaptation to the changing mechanical constraints during growth (adaptive juvenility).

Aims Ring width, specific gravity and specific modulus are important parameters for the mechanical stability of a standing tree. We aim at assessing whether their variations correspond to ontogenetic or adaptive juvenility.

Methods These parameters were measured at several positions across diametrical boards from 86 beech trees from 9 high forest stands. Their variance and correlations were analysed globally, between plots and between trees, and variations from pith to bark quantified according to the slope and curvature of radial profiles.

Results For the three parameters, the plot and tree effects were very significant, but within-tree variations were dominating, representing at least 50% of the total variance. These variations occurred both in the radial and the circumferential direction, as revealed by the frequency of non-symmetric diametral profiles. The patterns of radial variations were very diverse both between plots and within plots, being either increasing, decreasing or non-monotonous.

Conclusion Even if there is some ontogenetic influence in the measured juvenile patterns, their large variability suggests that adaptive juvenility dominates largely.

Keywords Variability, Radial variation, Core wood, Ontogenetic juvenility, Adaptive juvenility

Handling editor: Erwin Dreyer

This paper is a revised and edited version of the preprint available at https://hal.science/hal-04133248. The preprint was reviewed by two experts in the field and recommended by the Peer Community in Forest&Wood Sciences (https://forestwoodsci.peercommunityin.org/articles/rec?id=113) prior to submission to Annals of Forest Science, a PCI friendly journal. The editorial board of Annals of Forest Science took the recommendation into account and required some minor changes for clarity and adjustment to the format of the journal.

*Correspondence:
Joseph Gril
joseph.gril@cnrs.fr

[1] Laboratoire de Mécanique et Génie Civil, Montpellier, France
[2] Anhui Agricultural University, Hefei, China
[3] University of Montpellier, Montpellier, France
[4] Institut Pascal, Aubière, France
[5] Integrative Physics and Physiology of Fruit and Forest Trees, Clermont-Ferrand, France

© The Author(s) 2025. **Open Access** This article is licensed under a Creative Commons Attribution 4.0 International License, which permits use, sharing, adaptation, distribution and reproduction in any medium or format, as long as you give appropriate credit to the original author(s) and the source, provide a link to the Creative Commons licence, and indicate if changes were made. The images or other third party material in this article are included in the article's Creative Commons licence, unless indicated otherwise in a credit line to the material. If material is not included in the article's Creative Commons licence and your intended use is not permitted by statutory regulation or exceeds the permitted use, you will need to obtain permission directly from the copyright holder. To view a copy of this licence, visit http://creativecommons.org/licenses/by/4.0/.

1 Introduction

Wood is a material linked to the competition for height growth in the terrestrial environment, which is submitted to tremendous physical constraints such as gravity, wind and drought. The functions of wood (mechanical support, conduction and storage) respond to these constraints and are fulfilled by different cell types. In tree species, the bulk of wood material is generally made of dead, highly elongated cells, which have mainly a mechanical function: although they consist mostly of tracheids in softwoods and fibres in hardwoods, in the following they will be globally called "fibres". Despite their major importance for tree functioning and survival, other cell types (parenchyma, vessels in hardwoods) generally represent only a small part of the wood in terms of biomass investment. Actually, most of terrestrial biomass is in the form of fibres (Bar-On et al. 2018). This massive investment in fibres points to the major significance of the mechanical constraint for trees. The viewpoint that we will adopt here is that the amount and quality of wood products are mainly responses to the mechanical requirement for the tree in order to face the two major constraints that are wind and gravity.

Trees are built through wood growth (Thibaut 2019) including simultaneously primary growth by elongation or creation of twigs and secondary growth by thickening of existing axes. Secondary growth is performed by living wood cells in the cambial zone: stem cells of the cambium itself and daughter cells (Raven et al. 2007; Savidge 2003; Déjardin et al. 2010; Thibaut 2019). It consists of the following successive steps: division of the cambium stem cells into daughter cells; expansion of daughter cells until the end of primary wall formation; thickening of fibre and vessels cell walls until the end of secondary wall formation; lignification of the whole cell wall, including the compound middle lamella; programmed fibre and vessel cell death.

The cambial activity results in tree rings (in temperate tree species) and local wood properties that often differ from ring to ring. They can be described by ring width (*RW*), result of combined cell division and expansion, specific gravity (*SG*) resulting from the ratio between cell wall thickening and expansion, and specific modulus (*SM*) mainly determined by the organisation of the secondary cell wall (micro-fibril angle of the S2 layer) (Cave 1969). These three features determine most parameters involved in the adaptation to mechanical constraints. For a trunk of a given height, the rigidity against lateral wind forces depends on trunk diameter (related to *RW*) and on wood modulus of elasticity (MOE) which is the product of *SG* and *SM* (Fournier et al. 2013). For a given biomass investment, there is a trade-off between *RW* (large growth rate) and *SG* (large density). The flexibility of the trunk depends inversely on diameter, and positively on wood deformability (equal to the ratio of strength to modulus of elasticity, which is negatively correlated to *SM* as can be seen in wood databases, e.g. Ross 2010). The mechanical stability of the tree depends on its diameter, modulus of elasticity (product of *SG* by *SM*), and inversely on its green density (correlated to *SG*, Dlouha et al. 2018). The postural control (Alméras and Fournier 2009) depends on the asymmetry in radial growth rate (related to *RW*), modulus of elasticity, and maturation strain (often correlated to *SM*, Alméras et al. 2005). Mechanical adaptation is therefore a matter of fine-tuning of wood properties, and taking into account the trade-offs between them.

The secondary growth descriptors (*RW*, *SG*, *SM*) display spatial variation within a segment of the trunk, in the 3 cylindrical directions: transversely across radii (Tar), around the perimeter (Ap) and longitudinally along the stem (Las), called variation "TarApLas" within the tree by Savidge (2003). The variations around the perimeter in a given ring are related to posture control (Alméras and Fournier 2009), either due to trunk inclination (Alméras et al. 2005; Dassot et al. 2015) or to orientation change of the branches after apex death (Loup et al. 1991). In addition to the access to light, such peripheral modulations of properties can be related to the thigmomorphogenetic response of the stem to a dominant wind direction (Niez et al. 2020). The variations along the stem are related to primary growth: (i) succession of connected zones and free-from-branching portions of the axis and (ii) ageing of the terminal bud along the successive growth units. Apart from the vicinity of branching zones, these variations are rather slow (Savidge 2003).

Radial variations from pith to bark at a given height can be divided into two types: (i) intra-ring short-distance changes mostly due to seasonal effects and (ii) variations of mean ring properties, reflecting adaptations to changes in mechanical constraints during ontogeny. These mechanical constraints change according to the size of the tree (Fournier et al. 2013). The largest variations in dimensions and environment occur during the young ages. As a result, radial variations of these properties display larger gradients in the centre of a stem than in its periphery. This defines the "juvenile wood" also called "core wood"(Lachenbruch et al. 2011).

The steep radial variations in juvenile wood were nicely described by Bendtsen and Senft (1986). Loblolly pine (*Pinus taeda* L.) (Figs. 1 and 2) shows a typical radial pattern (TRP) of juvenility (Lachenbruch et al. 2011): initial increase of tracheid length, specific gravity (*SG*) and specific modulus (*SM*), initial decrease of ring width (*RW*). The initial segment with steep changes in properties corresponds to juvenile wood and is followed by rings with more stable properties called mature wood (which

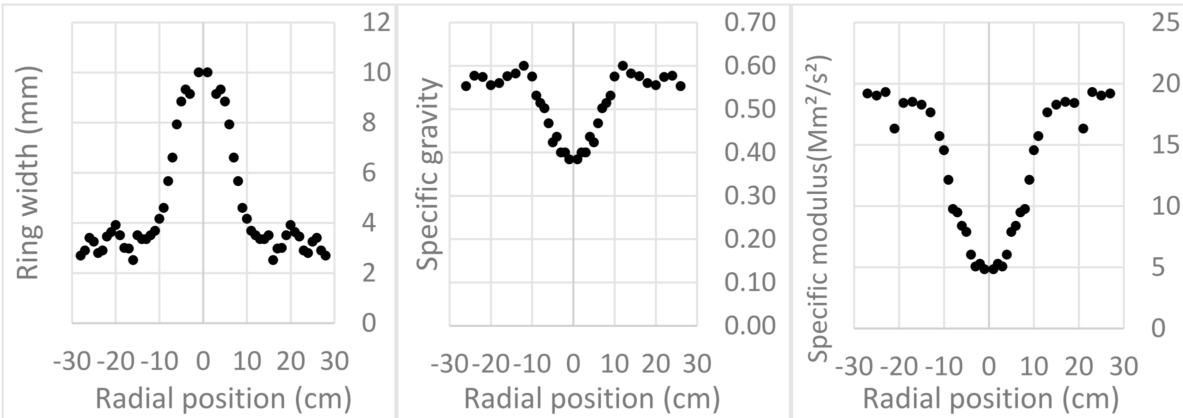

Fig. 1 Juvenility for mechanical indicators in Loblolly pine, after Bendtsen and Senft (1986): from pith to bark, according to the typical radial pattern, ring width decreases, specific gravity increases and specific modulus decreases

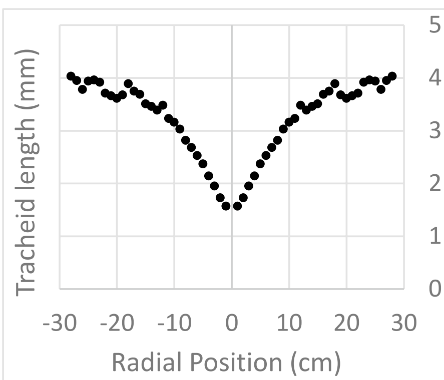

Fig. 2 Juvenility for tracheid length in Loblolly pine, after Bendtsen and Senft (1986): typical increase from pith to bark

nevertheless reveal interannual variations related to climate and mechanical constraints). Such patterns are generally observed in conifer plantations (softwood trees). (Cown and Dowling 2015, Larson et al. 2001).

Variations in tracheid or fibre length always share the same initial positive gradient for all trees (Fig. 2), whether softwood or hardwood (Koubaa et al. 1998; Larson et al. 2001; Bhat et al. 2001; Bao et al. 2001; Kojima et al. 2009). This parameter is important for the paper industry (Koubaa et al. 1998) but is only seldom cited as a factor influencing wood mechanical properties (Kollmann and Côté 1968; Kretschman 2010).

The variation of parameters characterising wood structure and properties depends on tree ontogeny and adaptation to changing constraints during its life. *Juvenility* describes the evolution of wood parameters during the early years of the stem. An important question is to separate the genetically programmed changes in properties with ontogeny (here termed *ontogenetic juvenility*) from the plastic adaptation to changing constraints (here termed *adaptive juvenility*). The systematic nature of juvenile gradients in fibre length suggests that they are a consequence of cambium ageing (ontogenetic juvenility). Here, we aim at investigating whether juvenile variations in three functional wood properties (*RW*, *SG* and *SM*) depend on plastic adaptation or on prescribed ontogenetic changes. It will be considered, for a given property, that ontogenetic changes are characterised by similar patterns of radial variations among a large sampling, while plastic adaptation corresponds to a large variability of radial patterns among trees and between populations.

For that aim, a sampling covering a wide diversity of geographical locations and forest management practices was required. The data obtained on a large panel of beech trees was exploited to characterise the patterns of radial variations of wood mechanical indicators in beech. Hypotheses that will be discussed are the following: (i) most of the variations are similar all around the trunk (profile symmetry); (ii) all the trees share the same radial pattern (ontogenetic juvenility) within the different growing conditions.

In healthy beech trees, heartwood and sapwood can scarcely be distinguished. A so-called red heartwood, which is a kind of chemical discolouration, is often observed (Liu et al. 2005) and affects the commercial value of the wood (Trenčiansky et al. 2017). The hypothesis that red wood occurrence does not affect mechanical parameters in tree rings will also be tested.

2 Material and methods

2.1 Material

Nine beech (*Fagus sylvatica* L.) plots representative of different forest managements were selected in Western

Table 1 Characteristics of the 9 plots from 9 different beech forest sites across Europe

Plot	1	2	3	4	5	6	7	8	9
Age (years)	120–140	~140	130	110	125	130	130–160	120	150–200
Altitude (m)	400	900	120	320	900	300	450	120	260–300
Country code	AT	AT	DK	FR	DE	DE	CH	CH	DE
Geographic coordinates	48°12′ N 16°10′ E	47°51′ N 16°10′ E	55°35′ N 12°04′ E	49°21′ N 06°02′ E	50°32′ N 09°25′ E	49°01′ N 09°13′ E	47°08.3′ N 08°17.1′ E	47°26′ N 07°03′ E	49°25′ N 09°21′ E
Forest type[a]	ea hf	ea hf (m)	ea hf	ea hf	ea hf	ea hf	uea hf	ea hf (m)	mhf
Nb trees	10	10	10	10	10	8	10	10	8
Height (m)	32.6	32.1	35.5	36.1	36	38.3	34	39.2	35.3
Slenderness (mm/m)	58.3	65	58.9	64	64.9	61.7	60.2	68	47.6
DBH (cm)	56	49.4	60.7	56.6	55.4	62.5	56.9	58.2	74.5

[a] *ea* even-aged, *uea* uneven-aged, *(m)* mountain, *hf* high forest, mhf: old middle forest transformed into even-aged high forest

Table 2 Mean, maximal, minimal values and coefficient of variation for height, slenderness and diameter at breast height of the 86 trees sampled in the 9 plots

86 trees	Mean	*Min*	*Max*	*C.V.*
Height (m)	35.4	23.7	42.6	10.1%
Slenderness (mm/m)	61.3	41.0	80.4	13.2%
Diameter (cm)	58.5	47.0	84.5	13.2%

Min minimum value, *max* maximum value, *C.V.* coefficient of variation

Europe (Becker and Beimgraben 2001; Jullien et al. 2013) (Table 1). Up to ten trees per plot (86 in total) were sampled for the measurement of wood properties (Table 1). All trees were dominant or co-dominant and their mean diameter at breast height was around 60 cm (Table 2).

One small 50 cm long log was cut at a height of 4 m for each tree. Each small log was cut into radial boards, through the pith, from North to South (North direction was carved in the log bark). These boards were air-dried to an average moisture content of 13.5% and cut into 1259 rods of 20 mm in radial, 20 mm in tangential and 360 mm in the longitudinal direction, from the pith outwards (Fig. 3). The rods with irregularities or cracks were discarded.

The rods were numbered according to their position in the board, their distance to pith was measured (note that the position in terms of ring number was not recorded in this study), and their orientation (North or South) was noted. At the same time, the number of rings at both ends of the samples was recorded and the mean annual ring width of the rod (*RW*) was calculated

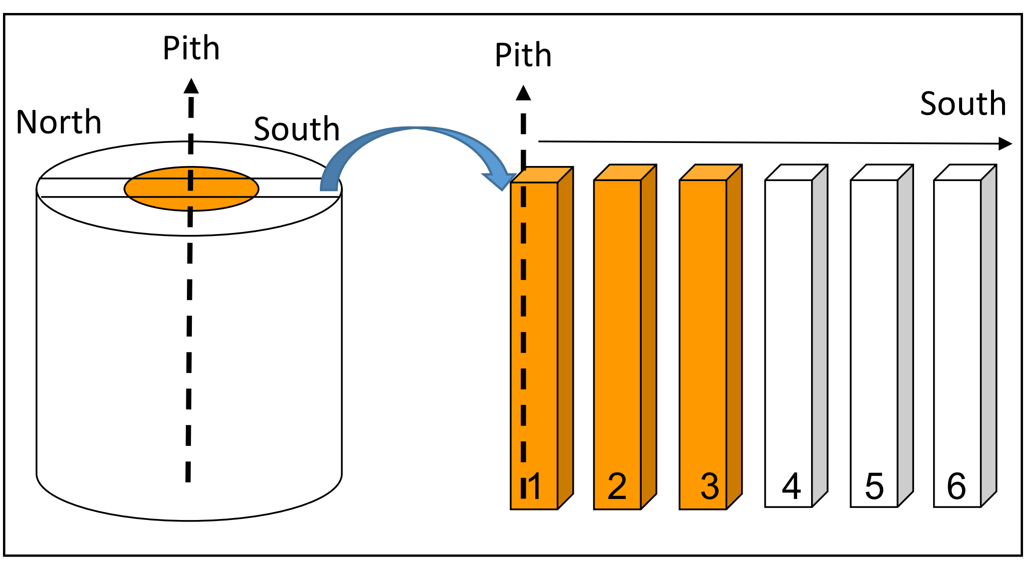

Fig. 3 Diagram of the sawing of the rod after the sawing of a North-South diametrical board. Numbering both for Northern and Southern parts of the board start with pith position. The coloured parts evoke the case of red heartwood occurrence

as the ratio of the mean radial dimension to the number of rings. Mean ring number per sample was 9.8, with a minimum of 3 and a maximum of 30. Each sample located at a distance lower than 10 cm from the pith was considered as a “core” sample. The presence of red heartwood was also noted for the rods located in the core (Liu et al. 2005).

2.2 Measurement of properties

Density (*D*) was calculated by measuring the weight (*W*) and the dimensions *R*, *T*, *L* of the rod: $D = W/(R.T.L)$. The specific gravity (*SG*) was the ratio between *D* and water density.

To measure the specific modulus (*SM*, 10^6m2/s2), each rod was positioned on fine wires and set in free vibration by a hammer stroke. The analysis of the sound vibration by fast Fourier transform gave the values of the three highest resonance frequencies, which were interpreted using equations yielding an estimate of *SM* where the contribution of longitudinal shear to the bending deformation has been eliminated (Brancheriau and Baillères 2002).

2.3 Statistical analyses

The measured wood properties (*RW*, *SG*, *SM*) are known to be strongly inter-correlated. Therefore, the distribution of properties and correlations between them were computed at various level (between rods, between trees and between plots).

2.3.1 Correlations and basic statistics

Basic statistical analyses were performed using the XLSTAT software. The normality of the distribution was verified by Shapiro-Wilk test. A Pearson correlation analysis was used in the case of a normal distribution, and a Spearman correlation analysis in the case of a non-normal distribution, which was the majority of cases.

2.3.2 Analysis of variance and variance components

Analyses of variance (ANOVA) and variance components analyses (VCA) were carried out using R software (R Core Team 2018). A first set of analyses tested the effect of the different factors on the three measured variables, using a nested ANOVA design where a random “tree” factor was nested within the “plot” factor, and the “core” factor nested within the “tree” factor. Sample orientation (North or South) was accounted for through an independent “orientation” factor.

Another set of ANOVA and VCA was carried out to test the effect of red heartwood on wood properties. This analysis was based only on core samples, as red heartwood occurs only on them. As both the measured properties and the occurrence of red heartwood were correlated to the distance to the pith, its effect was tested with a two-way ANOVA, with specimen number and red heartwood occurrence (Red) as two independent factors. A VCA was carried out on this model to quantify the share of variance of each factor.

2.3.3 Quantitative analysis of radial profiles

North and South radial profiles were analysed together, yielding 172 profiles on which the rod-averaged value of the three variables (*RW*, *SG* and *SM*) have been quantified as a function of the distance to the pith. We built a Microsoft Excel file to view and analyse these profiles (Alméras et al. 2024). The purpose of this analysis was the quantification of the shapes of these profiles, and how they correlate between properties or vary between plots. To achieve this, we considered two main indicators of each profile’s shape: the slope, and the curvature.

The slope of a particular radial profile was computed as the coefficient of the linear regression between the considered property and the distance to the pith. It indicates whether the property is globally increasing, decreasing, or staying constant. The curvature was computed as the coefficient of the quadratic term of a second-degree polynomial regression. A positive value corresponds to a convex shape, where the local slope increases outward, whereas a negative value corresponds to a concave shape, where the slope decreases outward. All combinations of slope and curvature can exist. Thus, each profile could be represented as a dot on a slope/curvature graph, corresponding to a particular shape. The correspondence between parameter’s values and profile shapes is illustrated in Fig. 4, where the ‘icons’ illustrate the symmetric shape corresponding to their position on the graph.

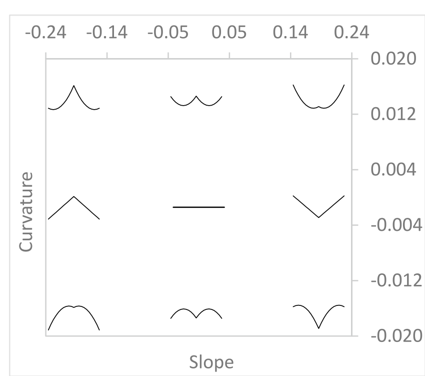

Fig. 4 Illustration of the correspondence between profile parameters (slope and curvature) and shape of a symmetric profile (“flying bird” icons)

The correlations between quantitative parameters of the profiles were analysed through a PCA (carried out using R) taking into account the following 15 variables for each of the 172 radial profiles: the mean value of the property (*RW_m*, *SG_m*, *SM_m*), the global slope (*RW_s*, *SG_s*, *SM_s*) obtained from the linear regression, the initial value of the property (*RW_a0*, *SG_a0*, *SM_a0*), the initial slope of the property (*RW_a1*, *SG_a1*, *SM_a1*) and the curvature (*RW_a2*, *SG_a2*, *SM_a2*), obtained as the coefficients of the second-degree polynomial regression.

At plot level, we computed the median and the interquartile range of each parameter (slope and curvature) on each variable (*RW*, *SG* and *SM*), to appreciate whether there were systematic differences in profile shapes between plots. An ANOVA was used to test the effect of the plot factor on each parameter.

The 172 profiles were then classified according to two criteria: they were classified as "Flat", "Up" or "Down" according to a threshold on the slope, and as "Straight", "Convex" or "Concave" according to a threshold on the curvature. We used a criterion based on the magnitude of the effect of each parameter rather than on its statistical significance. Indeed, in many cases, the significance of the slope (or curvature) was found high (low P-value) although the magnitude of the effect was weak when compared to the overall range of variation of the parameter. The threshold values were set at an arbitrary 50% of the overall standard deviation of each variable, scaled by the mean distance to the pith (10 cm) for the slope, and by its square for the curvature. At the tree level, the diametral profiles (including both North and South profiles) were classified as symmetric ("Sym") if the parameters of the North and South profiles differed less than a threshold defined consistently with above (Alméras et al. 2024).

3 Results

3.1 Effect of red heartwood on wood properties

The effect of red heartwood on wood properties was tested on core specimens only, accounting for the distance to the pith (specimen number) as an independent factor. The results (Table 3) show that the distance to the pith was always a significant factor while red heartwood was non-significant for *RW* and *SG*.

Contrary to our expectations, the effect of red heartwood on the specific modulus was significant, representing a substantial share of variance (8.6%). Its occurrence is associated to a lower *SM* ($-$ 0.67 10^6 m2/s2 in average, $-$3% of the mean value), even when the effect of distance to the pith was accounted for. Pöhler et al. (2006) found a significant difference (p<0.05) both for density and modulus of elasticity. But the two parameters were higher for red heartwood (+3% and +6% respectively, which means +3% for *SM*). One reason for the difference could be a modification of cell wall properties during the expansion of red heartwood. Another one could be that trees with lower *SM* were more prone to develop red heartwood in our sampling. Anyway, in both studies, the difference in density and specific modulus between red and white heartwood remained quite small. Therefore, it will not be considered in the following analysis.

Table 3 Results of the variance component analysis of the effect of red heartwood occurrence (Red) and specimen number (Num, indicating the distance to the pith) on the properties of core specimens: share of variance for each factor (%) and significance of the factors

Factor	*RW*	*SG*	*SM*
Num	2.5^{**}	2.7^{***}	3.0^{***}
Red	ns	ns	8.6^{***}

RW, ring width; *SG*, specific gravity; *SM*, specific modulus

*** $P<10^{-3}$; $^{**}P<10^{-2}$; ns P>0.05

3.2 Structuration of variance at the within-tree, between-tree and between-plot levels

ANOVA showed that plot, tree within plot and core within tree were all very highly significant factors ($P < 10^{-6}$) for the three measured variables (*RW*, *SG* and *SM*), while orientation was a significant factor only for *SM* (P = 0.00012). The share of variance of each factor for each variable is displayed in Table 4, together with the statistical significance of each factor. For *RW*, the core factor (inner 10 cm radius, compared to the outer zone) represented the largest fraction of variance, followed by the plot and tree factors. For *SG* and *SM*, the tree factor was the largest fraction of variance. The orientation factor was statistically significant only for *SM* with a very low

Table 4 Results of the variance component analysis of the effect of Plot, Tree, Core and Orientation factors on the properties of all specimens: share of variance for each factor (%) and significance of the factors

Factor	*RW*	*SG*	*SM*
Plot	21.9^{***}	14.0^{***}	15.4^{***}
Plot/tree	9.2^{***}	36.4^{***}	28.6^{***}
Plot/tree/core	29.5^{***}	18.2^{***}	14.6^{***}
Orientation	ns	ns	0.8^{***}
Error	39.4	31.4	40.6
Total	100	100	100
Total Within-Tree	68.9	49.6	56.0

RW ring width, *SG* specific gravity, *SM* specific modulus

*** $P<10^{-3}$; ns P>0.05

Table 5 Parameter description for the 1259 rods sampled from the 86 beech trees in the 9 plots

1259 rods	*RW*	*SG*	*SM*
Minimum	0.67	0.55	11.08
Maximum	6.67	0.83	27.49
Mean	2.30	0.69	22.22
Max/min	10.00	1.51	2.48
C.V.	35.0%	6.2%	10.9%

RW ring width (mm), *SG* specific gravity, *SM* specific modulus ($10^6 m^2/s^2$)

Table 6 Spearman correlation table between the three measured parameters, at rod level

1259 rods	*RW*	*SG*	*SM*
RW	1	0.16^{***}	-0.33^{***}
SG	0.16^{***}	1	0.12^{***}
SM	-0.33^{***}	0.12^{***}	1

RW ring width, *SG* specific gravity, *SM* specific modulus

*** $P<10^{-3}$; ns: $P>0.05$

Table 7 Parameter description for tree mean values

86 trees	*RW*	*SG*	*SM*
Minimum	1.29	0.63	17.6
Maximum	4.78	0.78	25.6
Mean	2.28	0.70	22.4
Max/min	3.70	1.24	1.46
C.V.	24.9%	4.8%	7.6%

RW ring width (mm), *SG* specific gravity, *SM* specific modulus ($10^6 m^2/s^2$)

share of variance and a very low difference in the mean value for North (637 rods; mean value = 22.1 10^6 m2/s2) and South (622 rods; mean value = 22.4 10^6 m2/s2).

3.3 Correlations between properties at different levels

3.3.1 Rod level

Table 5 shows descriptors of the distribution of properties for all samples (1259 rods). The variation of *SG* between samples was very low (coefficient of variation 6.2%) compared to that of *SM* (10.9%) and *RW* (35%).

SG and *SM* were correlated positively (Table 6). *RW* was correlated positively with *SG* and negatively with *SM*. These correlations were very significant although they explained only 5% to 10% of total variance.

3.3.2 Tree level

Table 7 shows the descriptors of the distribution of mean values of properties per tree. Variability at tree level, as quantified by the coefficients of variation, was significantly lower than at rod level, and notably low for *SG*. This result was consistent with the fact that a substantial part of the variance was at the within-tree level (Table 4, "Core" factor).

At the between-tree level, only the negative correlation between *RW* and *SM* remained significant (Table 8), showing that trees with higher growth rates (higher mean *RW*) had lower *SM*. Note that the correlation between these properties was even higher in magnitude at the tree level (– 0.40) than at the rod level (– 0.33), suggesting that the dependency of *SM* to the growth speed of a given tree does not result directly from a physical relation between wood properties.

Table 8 Spearman correlation table between the three measured parameters, at tree level

86 trees	*RW*	*SG*	*SM*
RW	**1**	0.08^{ns}	-0.40^{***}
SG	0.08^{ns}	**1**	0.16^{ns}
SM	-0.40^{***}	0.16^{ns}	**1**

RW ring width, *SG* specific gravity, *SM* specific modulus

*** $P<10^{-3}$; ns: $P>0.05$

Table 9 Parameter description for the 9 plots mean values

Plot	*RW*	*SG*	*SM*
1	2.06	0.70	21.5
2	1.80	0.71	23.1
3	2.63	0.70	22.2
4	2.50	0.71	21.2
5	2.12	0.68	21.9
6	2.57	0.73	23.7
7	2.84	0.68	22.0
8	1.63	0.68	24.1
9	2.50	0.67	21.7
Maximum	2.84	0.73	24.1
Minimum	1.63	0.67	21.2
Mean	2.29	0.70	22.4
C.V.	16.9%	2.6%	4.2%

RW ring width (mm), *SG* specific gravity, *SM* specific modulus ($10^6 m^2/s^2$)

Table 10 Spearman correlation table between the three measured parameters, at plot level

9 Plots	*RW*	*SG*	*SM*
RW	**1**	0.18^{ns}	-0.17^{ns}
SG	0.18^{ns}	**1**	0.23^{ns}
SM	-0.17^{ns}	0.23^{ns}	**1**

RW ring width, *SG* specific gravity, *SM* specific modulus

ns: $P>0.05$

3.3.3 Plot level

Table 9 shows the descriptors of the distribution of mean values of properties per plot. Variability at plot level was significantly lower than at tree level, consistent with the large part of variance at the between-tree level (Table 4, "Tree" factor).

At plot level, no correlation was detected between parameters (Table 10).

3.4 Diversity of radial profiles of properties

3.4.1 Illustration of profile diversity

A total of 516 profiles (86 trees × 2 orientations × 3 variables) were observed and analysed. The mean coefficient of determination ($R2$) of the regressions was 0.43 for the linear, and 0.61 for the second-degree polynomial regressions, showing that the quadratic term captured a large part of profile non-linearity.

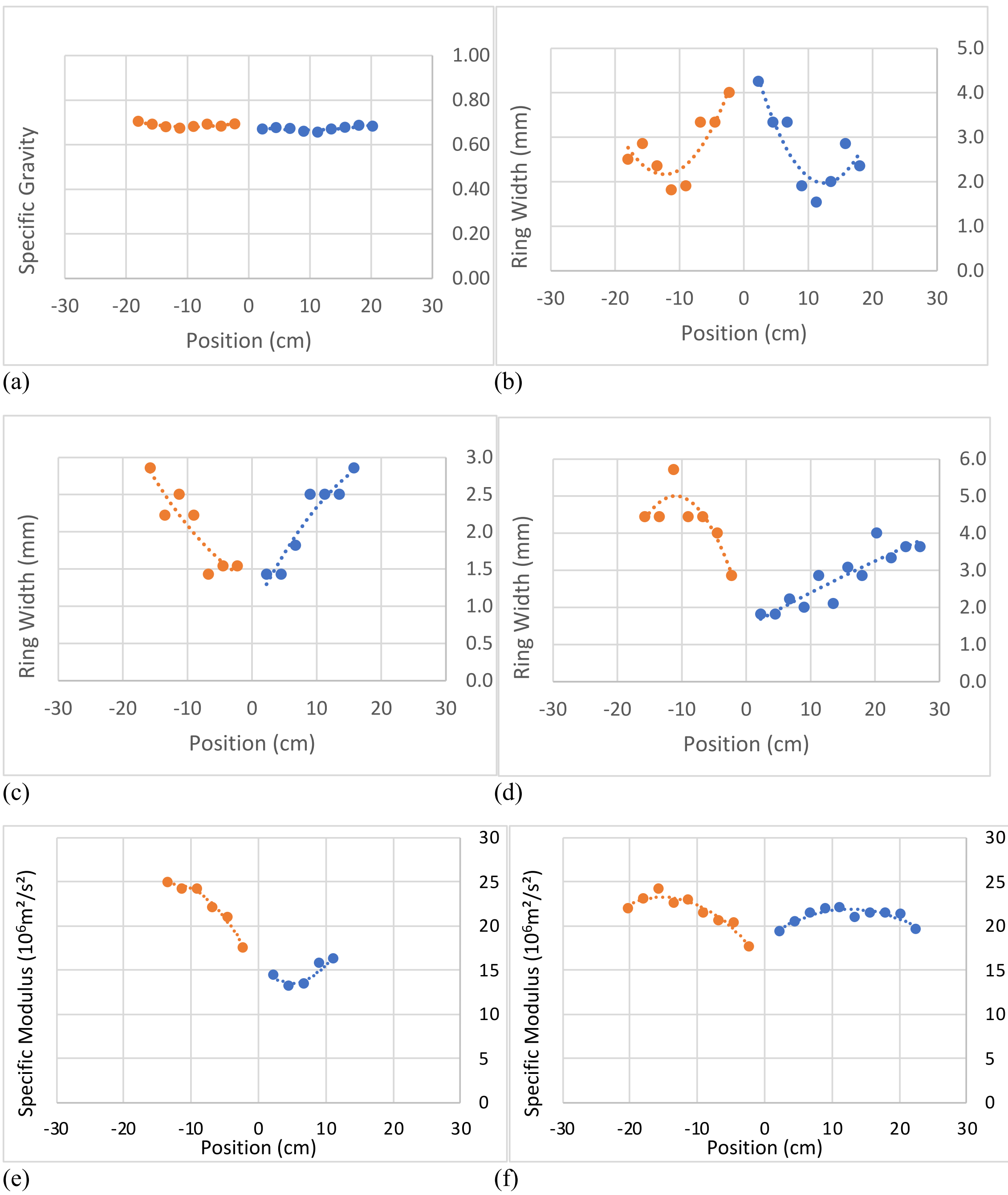

Fig. 5 Examples of property profiles: **a** tree 694, plot 6; **b** tree 443, plot 4; **c** tree 290, plot 2; **d** tree 1050, plot 9; **e** tree 1025, plot 9; **f** tree 299, plot 2

Examples of typical profiles together with the second-degree fitting are shown in Fig. 5 (all profiles can be viewed from the file provided by Alméras et al. (2024)). The chosen examples illustrate the diversity of the diametral profiles, with symmetric (a, b, c, e) as well as non-symmetric profiles (d, f). The radial profiles were either flat (a), increasing (c, d, e-South, f) or decreasing (b), and either straight (a, c, d-North), convex (b, f-North) or concave (d-South, e, f-South).

3.4.2 Typology of profiles

For each of the three studied variables, there was a large diversity of radial profiles, with instances of all nine possible combinations of slope ("Up", "Flat", "Down") and curvature ("Convex", "Straight", "Concave"). Nevertheless, the frequency of these different shapes differed (Table 11). The proportion of symmetric profiles ("Sym") was about one third, showing that most trees display substantial variations of properties around the periphery.

The proportion of flat radial profiles was about 40% for each variable. Most profiles were decreasing for *RW* and *SG*, and increasing for *SM*. But less than 50% of flat profiles were straight, meaning that most flat profiles were either convex (for *RW* or *SG*), or concave (as for *SM*) (Fig. 6).

The proportions of each type of profile seemed to differ among plots, as illustrated in Fig. 7.

3.4.3 Distribution of profile shape parameters

The median shape of all radial profiles is illustrated in Fig. 8. These profiles were "down-convex" for *RW* and *SG*, and "up-concave" for *SM*. The shape of the median profile of each plot can be viewed in Alméras et al. (2024).

The distribution of profile shape parameters (Fig. 9) shows that they were not randomly distributed. The plot effect on the slope parameter was significant for all three variables, while its effect on curvature was significant only for *SG*. A similar figure representing the distribution of parameters from individual radial profiles is provided by Alméras et al. (2024).

3.4.4 Correlations between profile-shape parameters

The correlations between profile-shape parameters are illustrated in Fig. 10. The first axis of this PCA opposes high initial ring width (*RW_a0*) and positive initial slope of specific modulus (*SM_a1*) to high initial specific modulus (*SM_a0*) and positive slope of ring width (*RW_a1*). This axis opposes high growth rate to high cell wall stiffness.

It is apparent that the initial slope (*_a1*) and curvature (*_a2*) were negatively correlated for all three variables: a faster initial change of a given variable is associated to a decreasing rate of change in the subsequent growth

4 Discussion

4.1 Interpretation of correlations between properties

Given the large difference in the variability of *SG* and *SM* (Table 5), the variability of the modulus of elasticity (the product of *SG* and *SM)*, is more dependent on the variations of *SM* than on the variations of *SG* in beech: The R^2 of the linear regression between MOE and SG is only

Table 11 Occurrence of profile types, characterised by the pattern of radial variation from pith to bark, for 172 North and South cases

N + S	Sym	Flat	Up	Down	Straight	Convex	Concave
RW	36%	41%	18%	41%	36%	37%	27%
SG	37%	42%	13%	45%	48%	34%	19%
SM	28%	42%	37%	20%	28%	10%	62%

RW ring width, *SG* specific gravity, *SM* specific modulus

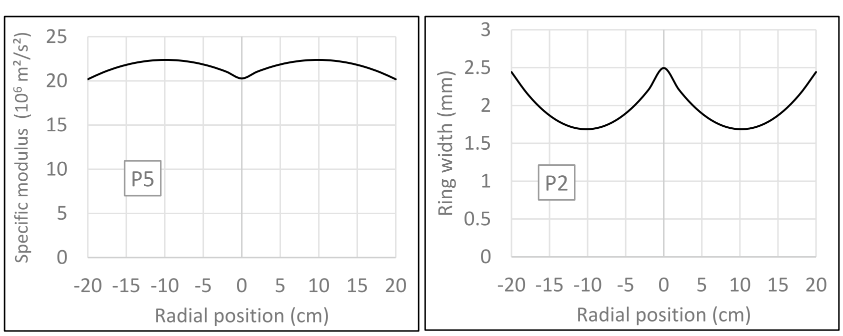

Fig. 6 Examples of median plot profiles with flat slope: flat-convex (specific modulus, plot 5) or flat-concave (ring width, plot 2)

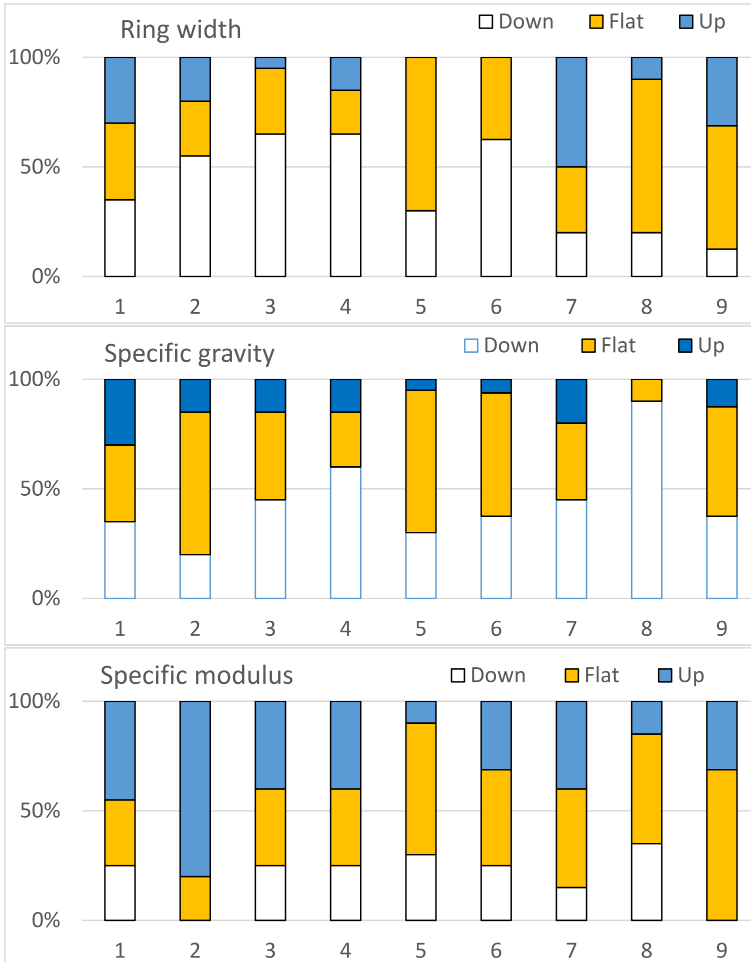

Fig. 7 Distribution of profile types for the 9 plots, based on the slope of the linear regression of the studied properties versus the radial position

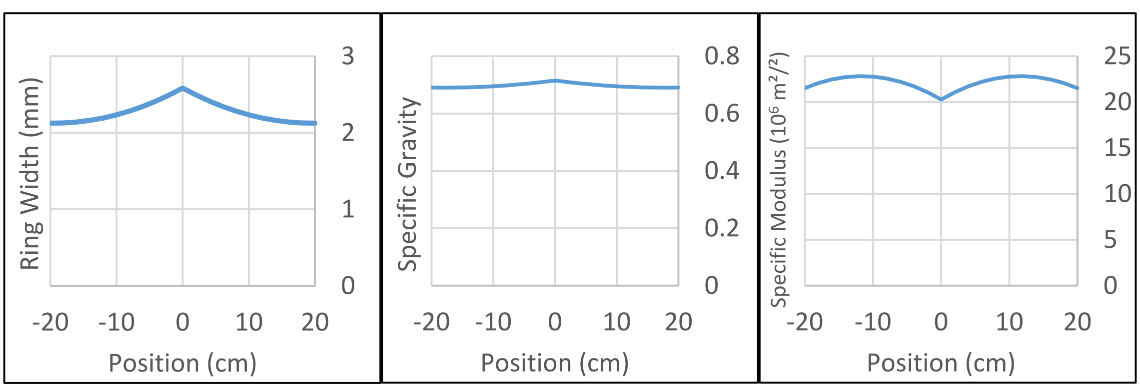

Fig.8 Median profiles over all trees, mixing both orientations in a symmetrical presentation

0.26, while that of the regression between SG and SM is 0.78.

Correlations between *RW* and both *SG* and *SM* were very highly significant, with a positive value for *SG* (density is higher for larger ring width) and a negative one for *SM* (specific modulus is lower for large rings). These results were partly due to covariations along the juvenility gradient that will be analysed in the next paragraph.

No correlation was detected between *SG* and *SM*. This can be interpreted as a global independence in

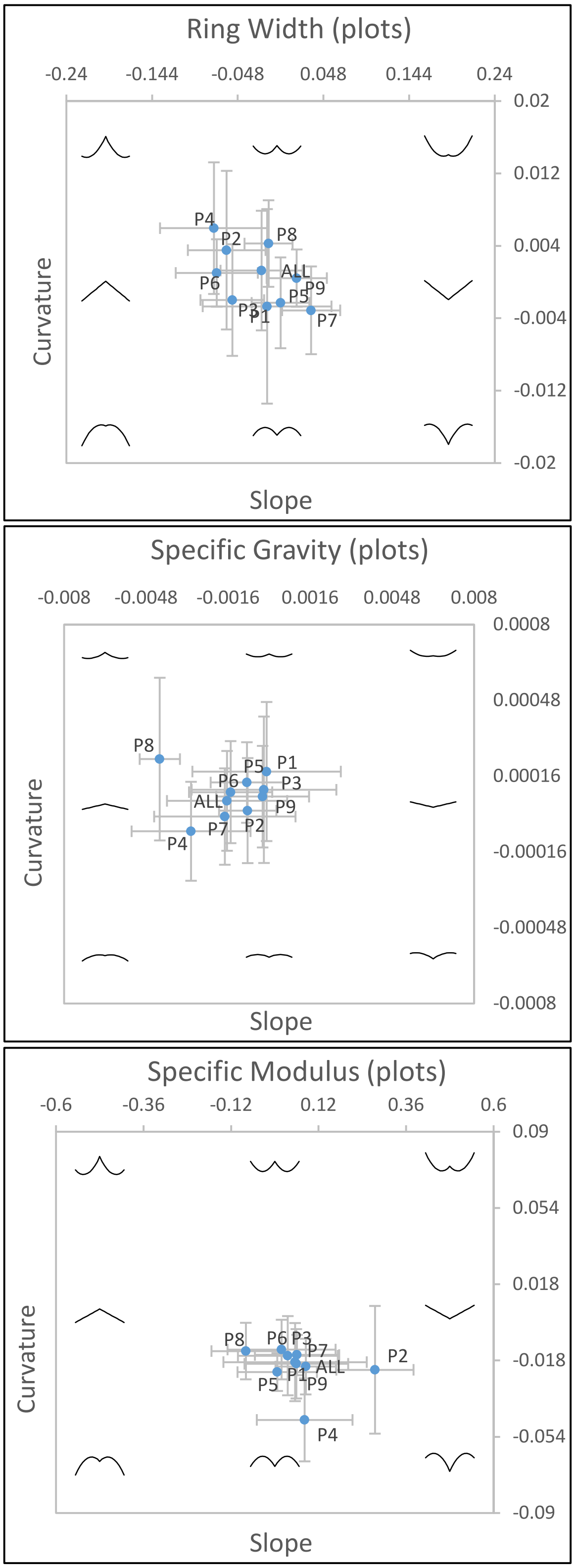

Fig. 9 Distribution of median plot profiles in the slope/curvature plane. Each panel represents the distribution (median and inter-quartile) of parameters (slope and curvature) for each plot. The figures are centred on zero on the *X*- and *Y*-axes, so that the centre of the figure represents the flat straight profile, and each quadrant of the figure represents a type of profile. "Flying-bird" icons represent the shape associated to their position in the figure (see also Fig. 4)

mechanical adaptation of the two parameters: *SG* reflects the quantity of cell wall (cell wall relative thickness), and *SM* its quality (microfibril angle), and these two parameters can be controlled independently during radial growth.

4.2 Major importance of within-tree variations in properties

The importance of within-tree variations can be deduced from Table 4. Within-tree variation is the share of variance that is not captured by higher scale factors ("Plot" and "Tree"), so it is the sum of the "Core" factor, the "Orientation" factor and the "Error" factor (Table 4). Within-tree variations represented approximately 65% of the variance for *RW*, 50% for *SG* and 55% for *SM*.

The within-tree variations of properties originated from both peripheral variations and radial variations. Peripheral variations were reflected by the frequent occurrence of non-symmetric diametral profiles: for all 3 variables, most trees presented important differences between North and South profiles (Table 11, Fig. 5). Radial variations were reflected by the importance of the "Core" effect (Table 4), and by the non-zero values of slope and curvature parameters of most radial profiles (Section 3.3.3).

4.3 The frequency of non-symmetric diametric profiles reveals the importance of the gravity constraint and posture control mechanisms

Most diametric profiles were asymmetric (Table 11) despite the fact that the "Orientation" factor had no systematic effect on wood properties (Table 4). This is because the tree asymmetry, if any, due to stem inclination (linked to the effect of wind or soil instability), asymmetric crown (linked to the adaptation to light availability), and/or prevailing winds, had only few reasons to be North/South. It is thus not surprising that no systematic effect of orientation was detected here.

Tree asymmetry induces mechanical constraints in relation to how trees manage gravity. Growth of an asymmetric tree induces a rapid increase of the bending moment applied by gravity to the trunk, which tends to bend the tree downwards. To counteract this effect, a gravitropic reaction is needed (Alméras and Fournier 2009; Gril et al. 2017). This reaction is

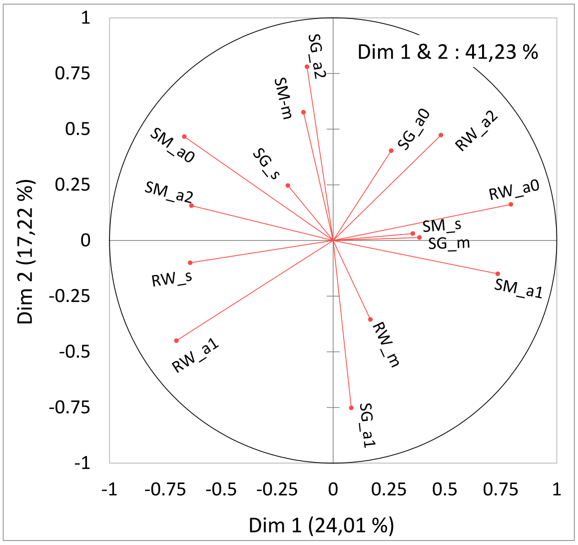

Fig. 10 Principal Component Analysis of shape profile parameters (dimensions 1 and 2: 41.23%). *RW*: ring width; *SG*: specific gravity; *SM*: specific modulus. _m: mean value of the property; _s: global slope obtained from the linear regression, _a0, _a1, _a2: initial value, initial slope and curvature, respectively, obtained as the coefficients of the second-degree polynomial regression

achieved by a dissymmetry of growth forces on the two sides of the inclined stem, with a higher tensile force on the upper side for hardwood species like beech. The tensile force produced on each side of the tree during wood maturation is proportional to ring width, to specific gravity, to specific modulus and to maturation strain (Alméras et al. 2005; Thibaut and Gril 2021). Increasing the force on the upper side means increasing the local value of any combination of these four factors, together with decreasing it on the lower side. This leads to asymmetric profiles of wood properties.

The occurrence of reaction wood is a typical expression of strong gravitropic reactions, influencing the asymmetry in *RW*, *SG*, *SM*, and in maturation strains, the latter resulting from macromolecular processes occurring during secondary wall formation (Alméras and Clair 2016; Thibaut and Gril 2021). However, for small inclination angles (e.g. coppice stems) the production of tension wood is not required: the difference in maturation strain between normal wood located on the lower and upper sides of the growing stem can be large enough for posture control (Thibaut and Gril 2021). The occurrence of tension wood is rather easy to detect by visual observation but variations of maturation strain in normal wood are, until now, impossible to estimate except by *in-situ* measurements of residual stress at stem periphery (Jullien et al. 2013).

4.4 Diversity in radial profiles suggests that "adaptive juvenility" is prevailing over "ontogenetic juvenility"

Most of the papers on the mechanical properties of juvenile wood refer to plantation trees, of softwoods or hardwoods (Bendtsen and Senft 1986; Kojima et al. 2009; Bhat et al. 2001; Bao et al. 2001). For softwoods, the "typical radial pattern" for mechanical factors (Lachenbruch et al. 2011) is always occurring in fast-growing plantations. It is characterised by a decrease of *RW* and an increase of both *SG* and *SM* from pith to bark until a juvenile core limit.

For hardwoods, this is not always the case, and *SG* can be more or less flat (Bendtsen and Senft 1986), while *SM* can be high near the pith and decrease for trees growing in dense tropical forests (Mc Lean et al. 2011). On *Bagassa guianensis* Aubl, a fast-growing secondary forest tree of French Guiana, Bossu et al. (2018) observed a typical radial pattern for microfibril angle and density, very clear for density (varying from 0.3 to 0.9 along the radius). Plourde et al. (2015) studied radial density variation for 91 tropical species (Costa Rica) and made the comparison for 74 species only: 42 over 74 (57%) had a net variation in density, 37 (88% of the 42) with increasing and 5 with decreasing radial pattern. Species from secondary forests (open environment in juvenile phase) displayed the clearest positive variations (low juvenile density), while in primary forests (closed environment during the juvenile phase) only anti-TRP species were found, with a lower variation (high internal density). Beech in this study is rather similar to trees from the primary forest with an internal density above 0.5 and a decreasing profile. Longuetaud et al. (2017) analysed 3 broadleaved trees: oak, beech, sycamore maple and two softwoods: fir and Douglas fir. The typical radial pattern was detected in maple and Douglas fir, but for oak, the density decreased instead of increasing. In fir and beech, the profile was bell-shaped (beech) or U-shaped (fir) with slight variations. Purba et al. (2021) studied density and microfibril angle in oak and beech for dominated, small-diameter trees harvested during thinning. Overall, the typical radial patterns applied to both cases.

For beech, we have measured parameters describing the juvenility in the wood of old trees in managed forests with a rather large diversity of sites and management practices. The median radial pattern for each parameter (Fig. 8) was similar to those described for some hardwoods in the literature for *SG*.

In Europe, old growth beech forests are submitted to different silviculture regimes (Ciancio et al. 2006): even-aged (France or Germany) or uneven-aged high forest (Switzerland), coppicing with standards (France) or conversion of coppiced forests into high forest (Germany, France). They however are never resulting from homogenous plantation regimes (none in the 9 plots). *Fagus* is known for its shade tolerance and ability to grow very slowly under a closed canopy (Collet et al. 2011) and most forest plots undergo more or less severe thinning before final harvesting, which leads to an increase of *RW* due to increased access to light (Noyer et al. 2017)—although a stronger thigmomorphogenetic response to wind could also exert some influence (Badel et al. 2015; Niez et al. 2020). This is reflected in the different mean radial patterns of *RW* among the 9 plots (Fig. 9). For plots 7 (uneven-aged high forest) and 9 (middle forest transformed into even-aged high forest), a clear increase of *RW* was observed in the young ages, while the reverse and classical pattern was detected in plots 1, 4, 5 and 6 (all even-aged forest in flat area). Similar results were found on younger beech trees (Bouriaud et al. 2004). The low *RW* values for plots 2 and 8 (even-aged, steep terrain) could be expected related to the specific conditions of climate, or soil, while the observed increase of *RW* after an initial decrease could possibly result from thinning operations in the young age.

Probably due to the large diversity of plot management, the beech median radial pattern did not apply to many trees. As a result, we observed no "universal" juvenile trend for any of the 3 parameters and we observed a large variety of radial patterns in each plot.

If the variation of wood properties had been governed by ontogenetic determinism, similar patterns would have been detected among trees and plots. The observed variability of radial patterns suggests, on the contrary, a dominance of plastic adaptation to mechanical constraints during tree growth (adaptive juvenility).

5 Conclusion

Based on the analysis of variance and of radial profiles, we showed that, for the 3 variables of concern (*RW*, *SG* and *SM*) within-tree variations represented the largest part of variance. These within-tree variations occurred both through peripheral variations (asymmetry between North and South profiles) and through radial variations (dependence of the property on the distance to the pith). The patterns of radial variations of the 3 variables were diverse, including increasing, flat and decreasing patterns, as well as convex, straight and concave patterns. Overall, these observations demonstrate that juvenile wood in Beech did not obey to systematic variations (ontogenetic juvenility), but was the result of plastic adaptation (adaptive juvenility) to variable individual trajectories and associated mechanical constraints.

One hypothesis that should be tested is the influence of change in access to light between trees of the same species in a similar environment, with very different initial growing conditions: (i) understorey beginning like in the primary forest, (ii) plantation at very high density, (iii) plantation at low density, using heliophilic, semi-tolerant and shade-tolerant species (Lehnebach et al. 2019). Measurement of radial variations of fibre length, ring width, basic specific gravity and specific modulus should be made with narrow spacing (each 2 mm) near the pith and larger ones (10 mm) nearer to the bark, in order to see if the transition between radial trend from one mode to the other is close to pith or not. Another study should be done on plantation trees with well-documented forest management: initial spacing (high and low), date and importance of thinning.

Moreover, modelling exercises should address growing trees with large differences in slenderness and radial evolution of specific gravity and specific modulus. Radial profiles of the maturation strain can be added with different hypotheses for a better representation of trunk growth. The tree stability (buckling or flexure risk) at each growing step could be documented.

Abbreviations

CV	Coefficient of variation
D	Density
L, *L*	Longitudinal direction, specimen length in L direction
R, *R*	Radial direction, specimen length in R direction
RW	Ring width
SG	Specific gravity (ratio of *D* over water density)
SM	Specific modulus (squared value of sound speed in L direction)
T, *T*	Tangential direction, specimen length in T direction
TRP	Typical radial pattern
W	Specimen weight

Authors' contributions

"BT managed the research project; SL, CL and DJ performed the measurements; BT prepared the first draft; TA made the final statistical analysis; BT, TA and JG prepared the final manuscript, DJ checked it"

Data availability

The datasets generated and analysed during the present study are accessible under the reference Alméras et al (2024) at : https://doi.org/10.5281/zenodo.14606666.

Declarations

Competing interests

The authors declare no competing interests.

Received: 29 January 2025 Accepted: 5 March 2025
Published online: 09 April 2025

References

Alméras T, Jullien D, Liu S, Loup C, Gril J and Thibaut B. (2024). Diversity of radial variations of wood properties in European beech reveals the plastic nature of juvenile wood. https://doi.org/10.5281/zenodo.14606666

Alméras T, Thibaut A, Gril J (2005) Effect of circumferential heterogeneity of wood maturation strain, modulus of elasticity and radial growth on the regulation of stem orientation in trees. Trees 19:457–467. https://doi.org/10.1007/s00468-005-0407-6

Alméras T, Fournier M (2009) Biomechanical design and long-term stability of trees: morphological and wood traits involved in the balance between weight increase and the gravitropic reaction. J Theor Biol. 256:370–381. https://doi.org/10.1016/j.jtbi.2008.10.011

Alméras T, Clair B (2016) Critical review on the mechanisms of maturation stress generation in trees. J Royal Soc Interface 13:20160550. https://doi.org/10.1098/rsif.2016.0550

Badel E, Ewers FW, Cochard H, Telewski FW (2015) Acclimation of mechanical and hydraulic functions in trees: Impact of the thigmomorphogenetic process. Front Plant Sci. 6:266. https://doi.org/10.3389/fpls.2015.00266 hal-01149365

Bao FC, Jiang ZH, Jiang XM, Lu XX, Luo XQ, Zhang SY (2001) Differences in wood properties between juvenile wood and mature wood in 10 species grown in China. Wood Sci Technol. 35:363–375. https://doi.org/10.1007/s002260100099

Bar-On YM, Phillips R, Milo R (2018) The biomass distribution on Earth. Proc Natl Acad Sci 115:6506–6511. https://doi.org/10.1073/pnas.1711842115

Bhat KM, Priya PB, Rugmini P (2001) Characterisation of juvenile wood in teak. Wood Sci Technol. 34:517–532. https://doi.org/10.1007/s002260000067

Becker G, Beimgraben T (2001) Occurrence and relevance of growth stresses in Beech (*Fagus sylvatica* L.) in Central Europe. Final Report of FAIR-project CT 98-3606, Coordinator Prof. G. Becker. Institut für Forstbenutzung und forstliche Arbeitwissenschaft, Albert-Ludwigs Universität, Freiburg

Bendtsen BA, Senft J (1986) Mechanical and anatomical properties in individual growth rings of plantation-grown eastern cottonwood and Loblolly pine. Wood Fiber Sci. 18:23–38

Bossu J, Lehnebach R, Corn S, Regazzi A, Beauchene J, Clair B (2018) Interlocked grain and density patterns in *Bagassa guianensis*: changes with ontogeny and mechanical consequences for trees. Trees 32:1643–1655. https://doi.org/10.1007/s00468-018-1740-x

Bouriaud O, Bréda N, Le Moguédec G, Nepveu G (2004) Modelling variability of wood specific gravity in beech as affected by ring age, radial growth and climate. Trees 18:264–276. https://doi.org/10.1007/s00468-003-0303-x

Brancheriau L, Baillères H (2002) Natural vibration analysis of wooden beams: a theoretical review. Wood Sci Technol. 36:347–365. https://doi.org/10.1007/s00226-002-0143-7

Cave ID (1969) The longitudinal Young's modulus of *Pinus radiata*. Wood Sci Technol. 3:40–48

Ciancio O, Corona P, Lamonaca A, Portoghesi L, Travaglini D (2006) Conversion of clearcut beech coppices into high forests with continuous cover: a case study in central Italy. For Ecol Manag. 224:235–240. https://doi.org/10.1016/j.foreco.2005.12.045

Collet C, Fournier M, Ningre F, Hounzandji AP, Constant T (2011) Growth and posture control strategies in *Fagus sylvatica* and *Acer pseudoplatanus* saplings in response to canopy disturbance. Ann Bot. 107:1345–1353. https://doi.org/10.1093/aob/mcr058

Cown D, Dowling L (2015) Juvenile wood and its implications. NZ J For. 59:10–17

Dassot M, Constant T, Ningre F, Fournier M (2015) Impact of stand density on tree morphology and growth stresses in young beech (*Fagus sylvatica* L.) stands. Trees 29:583–590. https://doi.org/10.1007/s00468-014-1137-4

Déjardin A, Laurans F, Arnaud D, Breton C, Pilate G, Leplé JC (2010) Wood formation in Angiosperms. C R Biol. 333:325–334

Dlouhá J, Alméras T, Beauchêne J, Clair B, Fournier M (2018) Biophysical dependences among functional wood traits. Funct Ecol. 32:2652–2665. https://doi.org/10.1111/1365-2435.13209

Fournier M, Dlouha J, Jaouen G, Alméras T (2013) Integrative biomechanics for tree ecology: beyond wood density and strength. J Exp Bot. 64:4793–4815. https://doi.org/10.1093/jxb/ert279

Gril J, Jullien D, Bardet S, Yamamoto H (2017) Tree growth stress and related problems. J Wood Sci. 63:411–432. https://doi.org/10.1007/s10086-017-1639-y

Jullien D, Widmann R, Loup C, Thibaut B (2013) Relationship between tree morphology and growth stress in mature European beech stands. Ann Forest Sci. 70:133–142. https://doi.org/10.1007/s13595-012-0247-7

Kojima M, Yamamoto H, Yoshida M, Ojio Y, Okumura K (2009) Maturation property of fast-growing hardwood plantation species: A view of fiber length. For Ecol Manag. 257:15–22. https://doi.org/10.1016/j.foreco.2008.08.012

Kollmann FFP, Côté AA (1968) Principles of wood Science and Technology. Springer-Verlag, I. Solid Wood. https://link.springer.com/book/10.1007/978-3-642-87928-9

Koubaa A, Hernandez RE, Baudouin M, Poliquin J (1998) Inter clonal, intra clonal and within-tree variation of fiber length of poplar hybrid clones. Wood Fiber Sci. 30(1):40–47

Kretschmann DE (2010) Mechanical properties of wood. In Wood handbook: Wood as an engineering material. General Technical Report FPL-GTR-190. Madison: Forest Products Laboratory, USDA, Forest Service

Lachenbruch B, Moore J, Evans R (2011) Radial variation in wood structure and function in woody plants, and hypotheses for its occurrence. In: Meinzer FC, Lachenbruch B, Dawson TE (eds) Size- and age-related changes in tree structure and function. Springer, Dordrecht, pp 121–164

Larson PR, Kretschmann DE, Clark AIII, Isebrands JG (2001) Formation and properties of juvenile wood in southern pines: a synopsis. Gen Tech Rep. FPL-GTR-129. US Department of Agriculture, Forest Service, Forest Products Laboratory, Madison, WI, p 42

Lehnebach R, Bossu J, Va S, Moel H, Amusant N, Nicolini E, Beauchêne J (2019) Wood density variations of legume trees in French Guiana along the shade tolerance continuum: heartwood effects on radial patterns and gradients. Forests 10:80. https://doi.org/10.3390/f10020080

Longuetaud F, Mothe F, Santenoise P, Diop N, Dlouha J, Fournier M, Deleuze C (2017) Patterns of within-stem variations in wood specific gravity and water content for five temperate tree species. Ann Forest Sci. 74:64. https://doi.org/10.1007/s13595-017-0657-7

Loup C, Fournier M, Chanson B (1991) Relations entre architecture mécanique et anatomie de l'arbre : cas d'un Pin maritime (*Pinus pinaster* Aiton). L'arbre, biologie et développement. Naturalia monspeliensa N° hors série (C. Edelin ed)

Liu S, Loup C, Gril J, Dumonceaud O, Thibaut A, Thibaut B (2005) Studies on European beech (*Fagus sylvatica* L.): variations of colour parameters. Ann. Forest Sci. 62:625–632. https://doi.org/10.1051/forest:2005063

Mc Lean JP, Zhang T, Bardet S, Beauchêne J, Thibaut A, Clair B, Thibaut B (2011) The decreasing radial wood stiffness pattern of some tropical trees growing in the primary forest is reversed and increases when they are grown in a plantation. Ann Forest Sci. 68:681–688. https://doi.org/10.1007/s13595-011-0085-z

Niez B, Dlouha J, Gril J, Ruelle J, Toussaint E, Moulia B, Badel E (2020) Mechanical properties of "flexure wood": compressive stresses in living trees improve the mechanical resilience of wood and its resistance to damage. Ann Forest Sci. 77:17. https://doi.org/10.1007/s13595-020-0926-8

Noyer E, Lachenbruch B, Dlouhá J, Collet C, Ruelle J, Ningre F, Fournier M (2017) Xylem traits in European beech (*Fagus sylvatica* L.) display a large plasticity in response to canopy release. Ann Forest Sci 74:46. https://doi.org/10.1007/s13595-017-0634-1

Plourde BT, Boukili VK, Chazdon RL (2015) Radial changes in wood specific gravity of tropical trees: inter- and intraspecific variation during secondary succession. Funct Ecol. 29:111–120. https://doi.org/10.1111/1365-2435.12305

Pöhler E, Klingner R, Künniger T (2006) Beech (*Fagus sylvatica* L.) - Technological properties, adhesion behaviour and colour stability with and without coatings of the red heartwood. Ann Forest Sci. 63:129–137. https://doi.org/10.1051/forest:2005105

Purba CYC, Dlouha J, Ruelle J, Fournier M (2021) Mechanical properties of secondary quality beech (*Fagus sylvatica* L.) and oak (*Quercus petraea* (Matt.) Liebl.) obtained from thinning, and their relationship to structural parameters. Ann Forest Sci 78:81. https://doi.org/10.1007/s13595-021-01103-x

R Core Team (2018) R: A language and environment for statistical computing. Vienna, R Foundation for Statistical Computing

Raven PH, Evert RF, Eichhorn SE (2007) The biology of plants. De Boeck, Brussels

Ross RJ (2010) Wood handbook: wood as an engineering material. USDA Forest Service, Forest Products Laboratory, General Technical Report FPL-GTR-190, 509 p. 1 v., 190

Savidge RA (2003) Tree growth and wood quality. In: Wood quality and its biological basis, edited by JR. Barnett and G. Jeronimidis, Blackwell scientific: Oxford (ISBN: 978-1-405-14781-1): 1-29

Thibaut B (2019) Three-dimensional printing, muscles and skeleton: mechanical functions of living wood. J Exp Bot. 70:3453–3466. https://doi.org/10.1093/jxb/erz153

Thibaut B, Gril J (2021) Tree growth forces and wood properties. Peer Community J 1:e46. https://doi.org/10.24072/pci.forestwoodsci.100006

Trenčiansky M, Lieskovský M, Merganič J, Šulek R (2017) Analysis and evaluation of the impact of stand age on the occurrence and metamorphosis of red heartwood. iForest 10:605–610. https://doi.org/10.3832/ifor2116-010

Publisher's Note

Springer Nature remains neutral with regard to jurisdictional claims in published maps and institutional affiliations.